



# Regioselective three-component synthesis and theoretical calculations of new alkane-linked bis(thiazol-2(3*H*)-imine) hybrids: a DFT-based FMO and local reactivity indices

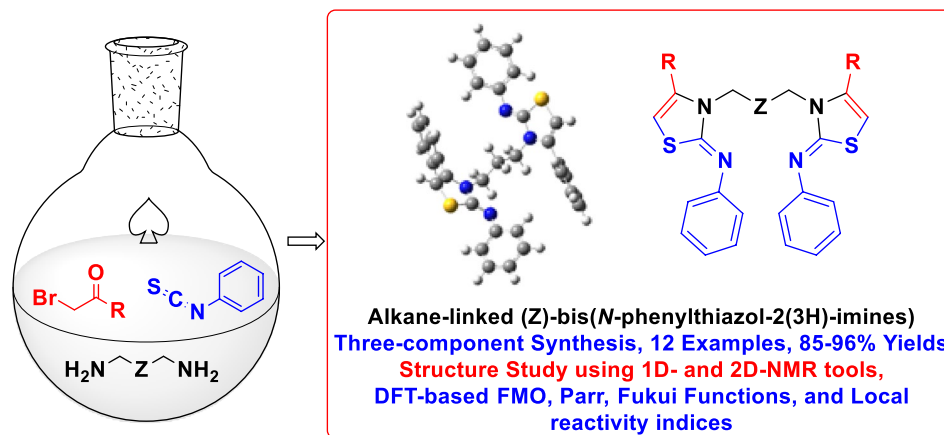
Mohamed S. Mohamed Ahmed<sup>1</sup> · Ahmed E. M. Mekky<sup>1</sup> · Sherif M. H. Sanad<sup>1</sup>

Received: 15 March 2023 / Accepted: 26 June 2023 / Published online: 19 July 2023  
© The Author(s) 2023

## Abstract

A three-component approach was conducted to adeptly prepare a new series of (*Z*)-bis(*N*-phenylthiazol-2(3*H*)-imines). The newly synthesized compounds were prepared by refluxing a ternary mixture of phenyl isothiocyanate, the suitable  $\alpha$ -bromoketones, and alkane-linked diamines in ethanol. Reaction conditions were optimized by comparing the yield of the final product under various bases, solvents, temperatures, and base-to-starting-materials molar ratios. The intended hybrids were produced with 85–96% yields while using ethanol at 80 °C for 3–5 h in the presence of anhydrous sodium acetate. The ascribed configuration of new products as well as the regioselectivity of the one-pot reaction were confirmed using both spectral data (1D and 2D NMR) and DFT-calculation techniques.

## Graphical abstract



**Keywords** DFT calculations · Local reactivity indices · Regioselective synthesis · Thiazol-2(3*H*)-imine · Three-component reactions

## Introduction

In a multicomponent reaction (MCR), at a minimum, three reactants are necessary, and most of the components from the beginning materials are incorporated into the final structures [1, 2]. The approach differs from multistep synthesis due to its high efficiency, simplicity, and cost-effectiveness in terms of the atoms and steps needed [3]. Mannich [4],

✉ Mohamed S. Mohamed Ahmed  
msmohamed@cu.edu.eg

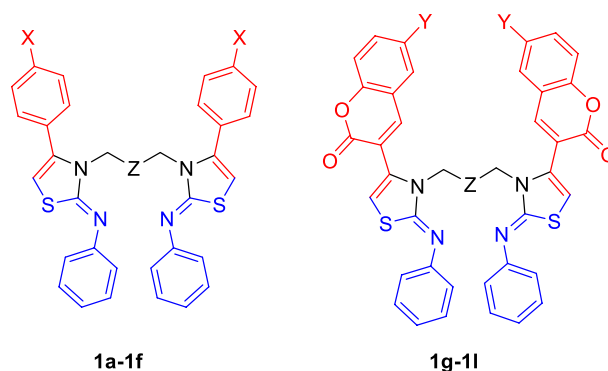
<sup>1</sup> Chemistry Department, Faculty of Science, Cairo University, Giza 12613, Egypt

Gewald [5], Povarov [6], Ugi [7], and Petasis [8] are only a few of the many multicomponent reactions with names of persons. Lately, similar procedures have been used to create molecular scaffolds with a variety of biological traits [9, 10].

Nitrogen-containing heterocycles showed a broad range of biological and pharmaceutical applications [11–14]. In particular, thiazol-2(3*H*)-imines demonstrate antibacterial [15], antifungal [16], fungicidal [17], analgesic [18], anti-inflammatory [19], anti-HIV [20], anticancer [21], and anti-proliferative activity [22]. Moreover, these hybrids have demonstrated potential as melanin-reducing (skin-whitening) agents [23], platelet GPIIb/IIIa receptor antagonists [19], antagonists of platelet GPIIb/IIIa receptors [18], inhibitors of acetylcholinesterase [24], inhibitors of GSK3 kinase, and inhibitors of MurB [11]. Figure 1 illustrates several chemicals with biological activity that contains an iminothiazole unit.

The 2-aminothiazole unit was first synthesized using the Hantzsch condensation reaction, which involved thiourea and  $\alpha$ -haloketones [25–28]. Later, using 1-substituted or 1,3-disubstituted thiourea derivatives, the method was used to synthesise *N*-substituted thiazol-2(3*H*)-imines [29–33]. Ionic liquids were used to facilitate the reaction by Shahvelayati et al. [34]. Kumar et al. also reported the synthesis of thiazol-2(3*H*)-imines in a one-pot reaction of amines and isothiocyanates with  $\beta$ -nitroacrylate [35] or (iodoethynyl) arene [36], which was generated in situ by arylacetylene oxy-iodination. *N*-alkylation of aminothiazoles [37], reaction of potassium thiocyanate with  $\alpha$ -bromoketimines [38], treatment of *N*-substituted thiourea derivatives with 3-bromomethyl-2-cyanocinnamionitrile [39, 40], and the cycloaddition-elimination reaction of 5-imino-1,2,4-thiadiazolidin-3-ones with dipolarophiles [41]. Other methods for efficiently preparing these hybrids have also been developed, such as the ring transformation of 1-arylmethyl-2-(thiocyanomethyl) aziridines [42], and the reaction of *N*-propargylaniline with acylisothiocyanates [43].

We present herein a three-component procedure for the synthesis of various regioisomeric alkane-linked bis(thiazol-2(3*H*)-imine) hybrids **1** that are attached to arene or chromene units as part of our ongoing efforts to produce azoles (see Fig. 2) [44–50]. 1D and 2D NMR spectroscopy were used to determine the structures of the resulting



**Fig. 2** Structure of the target regioisomeric alkane-linked bis(thiazol-2(3*H*)-imine) hybrids **1**

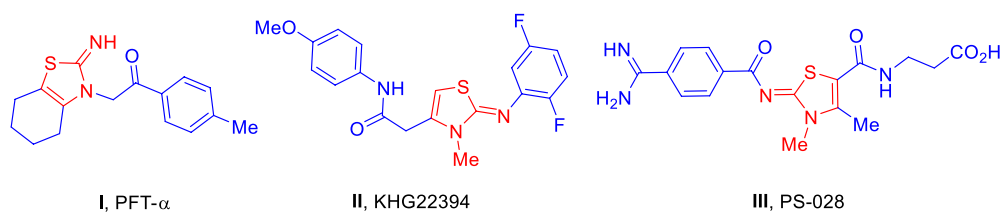
products. DFT has proven to be an effective tool for determining chemical reactivity and reaction mechanisms in both organic and inorganic chemistry [51, 52]. DFT calculations were also carried out to gain insight into the structures of the target thiazoles and the mechanism of their formation.

## Results and discussion

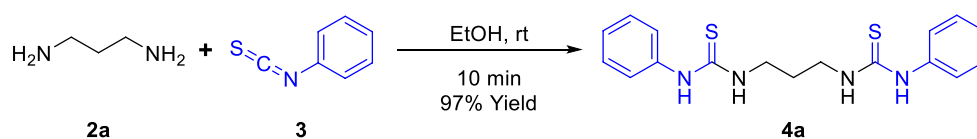
### Chemistry

The synthon propane-linked bis(3-phenylthiourea) **4a** was formed by reacting propane-1,3-diamine **2a** in a 1:2 ratio with phenyl isothiocyanate **3**. The resulting mixture was stirred in ethanol for 10 min at room temperature (rt) to yield **4a** with a 97% yield (see Scheme 1) [53].

The synthetic potential of bis(3-phenylthiourea) **4a** was then investigated and evaluated through its reaction with an ethanolic solution of 2-bromo-1-(4-methoxyphenyl)ethan-1-one **5c** in the presence of triethylamine (TEA) at 80 °C. TLC analysis revealed that after 3 h of heating, the reaction produced a single product, which was then isolated with an 80% yield. The previous product could be assigned to one of two regioisomeric structures, bis(*N*-phenylthiazol-2(3*H*)-imine) derivative **1c** or bis(3-phenylthiazol-2(3*H*)-imine) derivative **6c** (see Scheme 2).

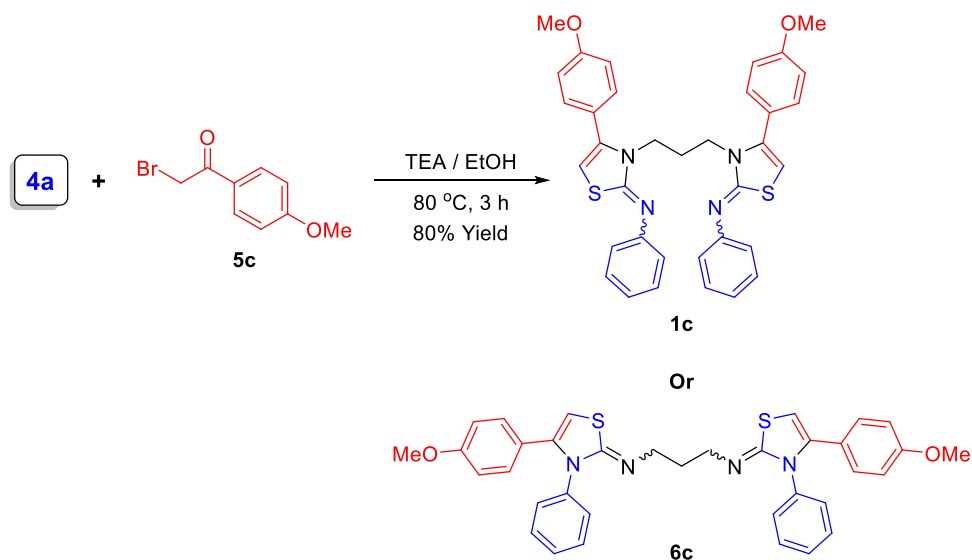


**Fig. 1** Some biologically active iminothiazole-based scaffolds



**Scheme 1** Synthesis of propane-linked bis(3-phenylthiourea) **4a**

**Scheme 2** Synthesis of the regioisomeric products bis(thiazol-2(3*H*)-imine) derivative **1c** or **6c**



Elemental analysis and spectral data were used to deduce the structure of the previous product. The  $^1\text{H-NMR}$  spectrum of such a product revealed two broad singlet signals at  $\delta$  1.85 and 3.67 corresponding to propane spacer protons, as well as two singlet signals at  $\delta$  3.78 and 6.02 corresponding to OMe and thiazole-H protons. It also revealed a multiplet signal at  $\delta$  6.93–7.32, which was attributed to 18 aromatic protons. The isolated product's  $^1\text{H-}^1\text{H}$  NOESY spectrum provided additional evidence for its structure (see Fig. 3).

Due to the absence of cross-peaks between NPh-H2 and aryl-H2 protons, the structure of the isolated product was assigned as bis(*N*-phenylthiazol-2(3*H*)-imine) derivative **1c** and the alternative regioisomeric product bis(3-phenylthiazol-2(3*H*)-imine) derivative **6c** was ruled out (see Fig. 4).

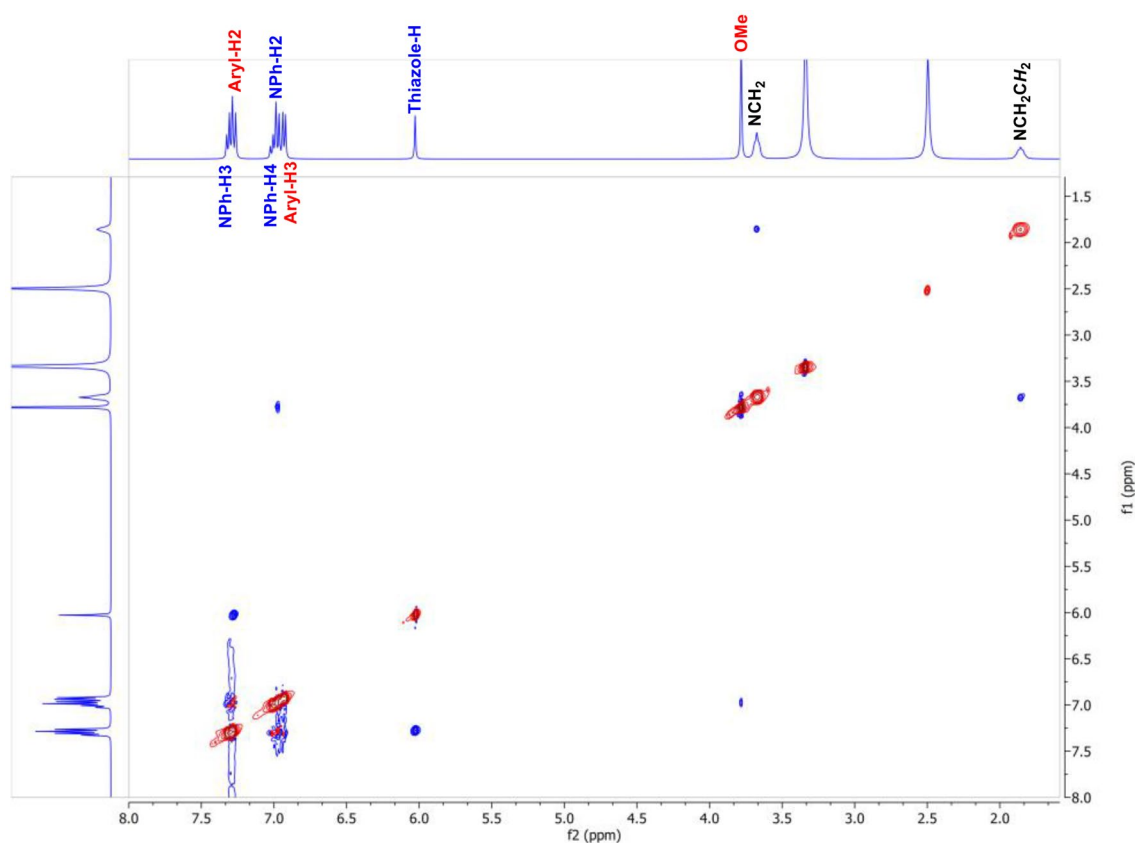
Compound **1c**'s  $^1\text{H-}^1\text{H}$  NOESY spectrum provided additional evidence for its presence in a (*Z*)-configuration (see Fig. 5). The presence of **1c** in an (*E*)-configuration is ruled out because there are no cross-peaks between NPh-H2 and the propane spacer. This finding is consistent with the previous X-ray single crystal study on (*Z*)-4-methyl-*N*,3-diphenylthiazol-2(3*H*)-imine reported by Murru et al. [54].

We continued our efforts, inspired by the findings, to prepare the target bis(*N*-phenylthiazol-2(3*H*)-imines) **1** using a one-pot protocol. The synthesis of **1c** was taken as a model. A ternary mixture of propane-1,3-diamine **2a**, phenyl isothiocyanate **3**, and 2-bromo-1-(4-methoxyphenyl)ethan-1-one **5c** was reacted in various solvents and bases (see Scheme 3

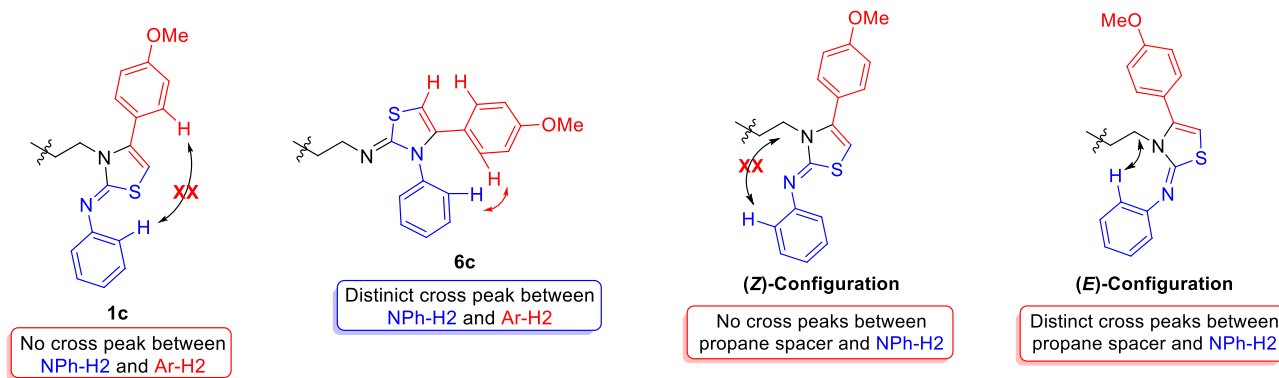
and Table 1). All reactions were monitored by TLC analyses. The potential of TEA or diethylamine (DEA) was investigated. As a result, using two equivalents of each base, TEA and DEA were tested in various solvents, such as ethanol at 80 °C, dioxane at 100 °C, and toluene at 80 °C (Table 1, Entries 1–6). The previous conditions produced the target **1c** in 52–80% yields.

It is worth of mention that our first attempt to start the one-pot synthesis of **1c** in the presence of DEA resulted in the formation of a mixture of several products, as detected by TLC analysis. This could be due to the side reaction of DEA with phenyl isothiocyanate **3**, which interferes with the formation of the bis(3-phenylthiourea) **4a**. To avoid this, propane-1,3-diamine **2a** was reacted first with two equivalents of phenyl isothiocyanate **3** at rt in the respective solvent. After 10 min of stirring, the intermediate **4a** was completely formed, and then two equivalents of both **5c** and DEA were added to the reaction mixture to complete the formation of target **1c**.

Moreover, the use of two equivalents of sodium bicarbonate, sodium carbonate, potassium carbonate, or cesium carbonate to mediate such three-component reactions in ethanol at 80 °C or dioxane at 100 °C was investigated. These inorganic bases produced **1c** in yields ranging from 58 to 81% (Table 1, Entries 7–14). Furthermore, the use of two equivalents of anhydrous sodium acetate was examined. At temperatures ranging from 40 to 80 °C, an



**Fig. 3** The  $^1\text{H}$ - $^1\text{H}$  NOESY spectrum of the regioisomeric products bis(thiazol-2(3H)-imine) **1c** or **6c**

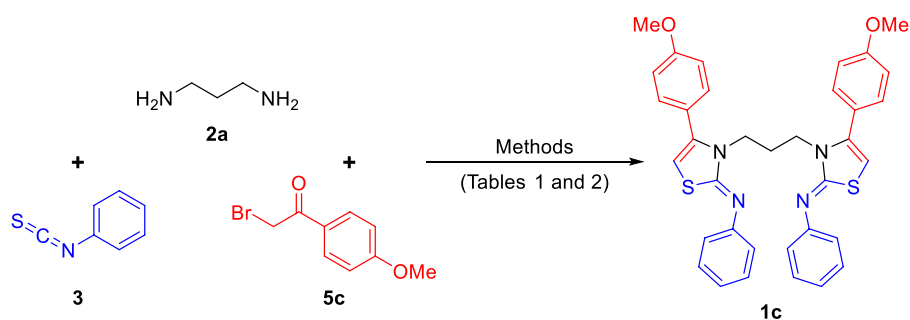


**Fig. 4** The diagnostic correlation of the  $^1\text{H}$ - $^1\text{H}$  NOESY for the regioisomeric products **1c** or **6c**

**Fig. 5** The diagnostic correlation of the  $^1\text{H}$ - $^1\text{H}$  NOESY for the (*E*)-/*(Z)*-configuration of **1c**

ethanolic sodium acetate solution was used to mediate the one-pot reaction. The reaction yielded **1c** in 60 and 79% yields at 40 and 60 °C, respectively (Table 1, Entries 15 and 16). The best yield, 87% of **1c**, was obtained using ethanol at 80 °C (Table 1, Entry 17). Also, the use of dioxane at 70 and 100 °C was investigated to give **1c** in 71 and 83% yields, respectively (Table 1, Entries 18 and 19).

Following that, the amount of anhydrous sodium acetate required to mediate the three-component synthesis of **1c** was investigated (see Table 2). All reactions were carried out in ethanol for 2–4 h at 80 °C with sodium acetate amounts ranging from 2 to 2.5 equivalents. For the one-pot protocol, the best reaction conditions were 2.2 equivalents of sodium acetate for 3 h. It yielded **1c** with a 95% yield (Table 2 and Entry 4).

**Scheme 3** One pot synthesis of bis(*N*-phenylthiazol-2(*3H*)-imine) derivative **1c****Table 1** Optimizing the one-pot synthesis of bis(*N*-phenylthiazol-2(*3H*)-imine) **1c** using two equivalents of the respective base

Entry	Base	Solvent	Temp. (°C)	Time (h)	Isolated yield (%)
1	TEA	EtOH	80	4	80
2	TEA	Dioxane	100	4	72
3	TEA	Toluene	80	4	55
4	DEA	EtOH	80	4	71
5	DEA	Dioxane	100	4	65
6	DEA	Toluene	80	4	52
7	NaHCO <sub>3</sub>	EtOH	80	4	69
8	NaHCO <sub>3</sub>	Dioxane	100	4	65
9	Na <sub>2</sub> CO <sub>3</sub>	EtOH	80	4	77
10	Na <sub>2</sub> CO <sub>3</sub>	Dioxane	100	4	72
11	K <sub>2</sub> CO <sub>3</sub>	EtOH	80	4	81
12	K <sub>2</sub> CO <sub>3</sub>	Dioxane	100	4	75
13	Cs <sub>2</sub> CO <sub>3</sub>	EtOH	80	4	62
14	Cs <sub>2</sub> CO <sub>3</sub>	Dioxane	100	4	58
15	NaOAc	EtOH	40	8	60
16	NaOAc	EtOH	60	6	79
17	NaOAc	EtOH	80	4	87
18	NaOAc	Dioxane	70	6	71
19	NaOAc	Dioxane	100	4	83

**Table 2** Optimizing the yield of sodium acetate-mediated synthesis of bis(*N*-phenylthiazol-2(*3H*)-imine) **1c**

Entry	Equivalents	Time (h)	Yield (%)
1	2	4	87
2	2.1	4	90
3	2.2	2	93
4	2.2	3	95
5	2.2	4	94
6	2.3	3	94
7	2.3	4	92
8	2.4	4	92
9	2.5	4	91

The research was then expanded to produce a series of alkane-linked bis(*N*-phenylthiazol-2(*3H*)-imines) **1a–1f**. The desired hybrids were created with minor modifications to the optimized one-pot protocol. After heating the respective reaction mixture at 80 °C for 3–4 h, the appropriate alkane-linked diamines **2a,b**, and *p*-substituted phenacyl bromides **5a–5c** were used to produce the target products **1a–1f** in 89–96% yields (see Scheme 4) [31].

The previous one-pot reaction was also investigated with the appropriate 3-(2-bromoacetyl)-2*H*-chromen-2-ones **5d–5f**. Additional six hybrids of bis(*N*-phenylthiazol-2(*3H*)-imines) **1g–1i** linked to chromene units were obtained in 85–91% yields after 4–5 h of heating at 80 °C (see Scheme 5) [55].

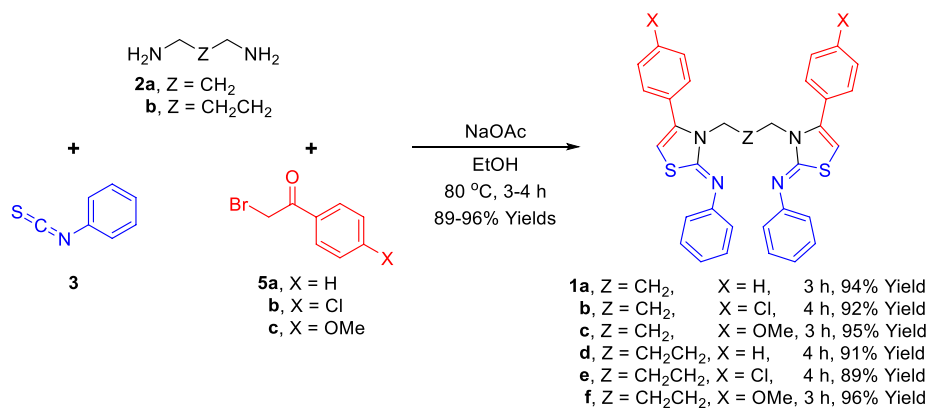
## Quantum chemical calculations

### Frontier molecular orbitals (FMO) calculations

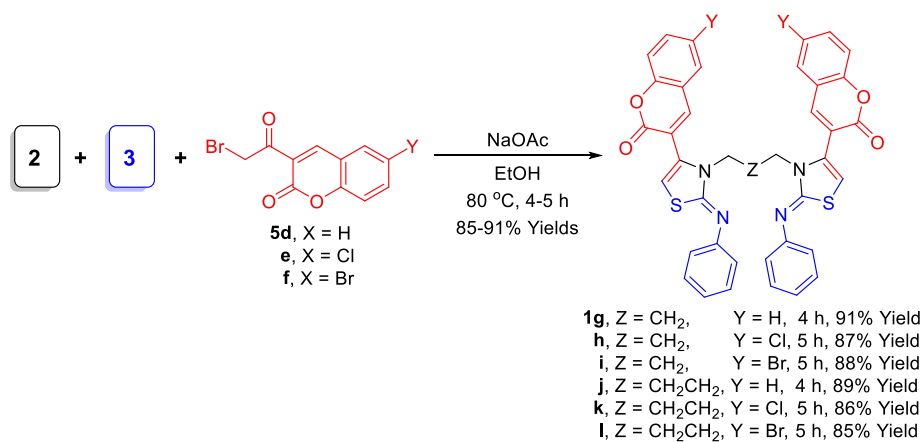
**FMO computations for the  $\alpha$ -haloketone 5 and bis(carbamimidothioates) 7/8** The use of quantum chemical algorithms has made tracing reaction mechanisms easier. Theoretical calculations were used herein to determine the best reaction product for a three-component reaction involving alkane-linked diamines **2**, phenyl isothiocyanate **3**, and  $\alpha$ -bromoketones **5**. As previously stated, bis(3-phenylthiourea) derivatives **4** were prepared in the first step of this reaction. When exposed to sodium acetate, these intermediates could potentially convert into one of four (*Z/E*)-bis(carbamimidothioates) **7** or **8**. (shown in Scheme 6). Following the reaction of (*Z/E*)-bis(carbamimidothioates) **7** or **8** with  $\alpha$ -bromoketones **5**, the regioisomeric (*Z/E*)-bis(thiazol-2(*3H*)-imines) **1** or **6** are formed.

The optimized structures of  $\alpha$ -bromoketones **5** and (*Z/E*)-bis(carbamimidothioates) **7/8** were generated using DFT (B3LYP/6–31 + G) computations with the Gaussian 09 program and presented in Gauss view 6.0.16. [56–58] The energies of **5** and **7/8**, along with the general characteristics of each compound, are summarized in Tables 3 and 4, respectively.

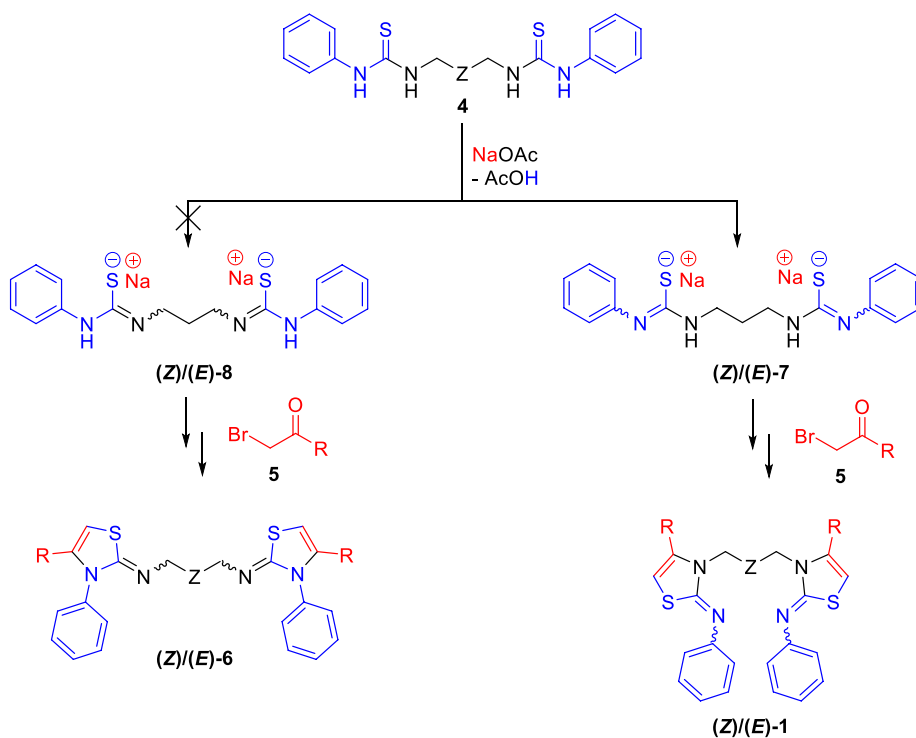
**Scheme 4** One pot synthesis of alkane-linked bis(*N*-phenylthiazol-2(3*H*)-imines) **1a–1f**



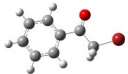
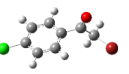
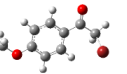
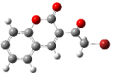
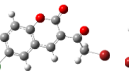
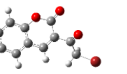
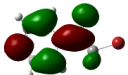
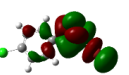
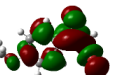
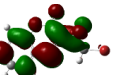
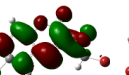
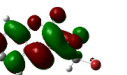
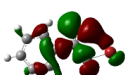
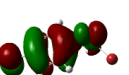
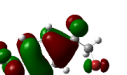
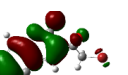
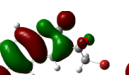
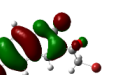
**Scheme 5** One pot synthesis of chromene-linked bis(*N*-phenylthiazol-2(3*H*)-imines) **1g–1l**



**Scheme 6** Formation of alkane-linked bis(carbamimidothioates) **7/8**



**Table 3** FMO of  $\alpha$ -bromoketones **5**

Reactant	<b>5a</b>	<b>5b</b>	<b>5c</b>	<b>5d</b>	<b>5e</b>	<b>5f</b>
Optimized structure						
LUMO						
$E_{\text{LUMO}}$ (eV)	-2.552	-2.645	-2.211	-3.113	-3.302	-3.309
HOMO						
$E_{\text{HOMO}}$ (eV)	-7.374	-7.410	-6.708	-7.155	-7.181	-7.130

**Global descriptors of the  $\alpha$ -haloketone **5** and bis(carbamimidothioates) **7/8**** Global descriptors for **5** and **7/8** are listed in Table 5, including nucleophilicity, electrophilicity, and total energy. Table 5 demonstrates that bis(carbamimidothioates) **7** are more favored than regioisomeric **8**. It was also discovered that the *Z*-forms were preferred over the *E*-forms [59]. Specifically, the total energy values of (*Z/E*)-**7a** were -1,254,254.710 and -1,254,249.402 kcal/mol, respectively, while those of (*Z/E*)-**8a** were -1,254,230.28 and -1,254,214.504 kcal/mol, respectively. Similarly, (*Z/E*)-**7b** had total energy values of -1,278,912.874 and -1,278,911.847 kcal/mol, respectively, whereas those of (*Z/E*)-**8b** had values of -1,278,900.831 and -1,278,900.322 kcal/mol, respectively. Based on these results, it can be concluded that the formation of (*Z*)-**7a** and (*Z*)-**7b** are the most probable intermediates for the one-pot reaction investigated in this study. These findings are supported by the data collected by 2D-NMR, which indicates the formation of the regioisomeric (*Z*)-bis(thiazol-2(3*H*)-imines) **1**.

In addition, we conducted a screening of the nucleophilicity and electrophilicity of both reactants and found that intermediates **7** act as nucleophilic species, while  $\alpha$ -bromoketones **5** act as electrophilic species. For instance, **7a** exhibits a nucleophilicity of 4.504, which is higher than **5a**'s value of 2.034. In contrast, the electrophilicity of **7a** is 1.149, which is lower than **5a**'s value of 2.554. This indicates that **7a** will attack **5a** during the reaction, with electrons moving from **7a** to **5a**.

**FMO calculations for the possible products (*Z/E*)-**1**** DFT at (B3LYP/6-31G) level was used to shed more light on the correct configuration of the regioisomeric products **1** [56–58]. Table 6 shows the visualized optimized structures, HOMO, and LUMO of products (*Z/E*)-**1a**, as well as their energies in three different media, namely gas, water, and ethanol. All findings are presented in Tables S1 and S2 in the electronic supplementary file.

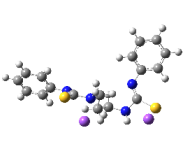
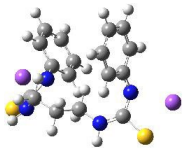
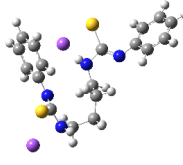
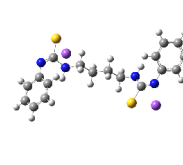
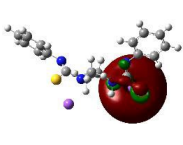
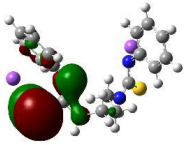
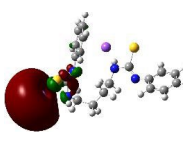
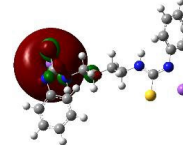
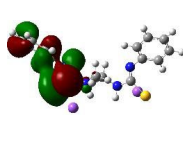
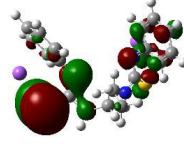
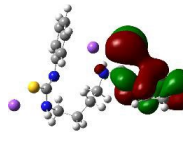
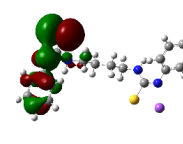

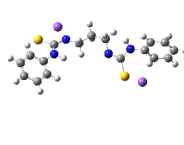
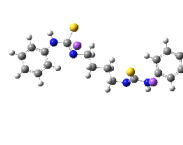
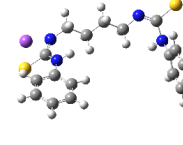

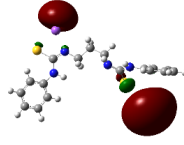
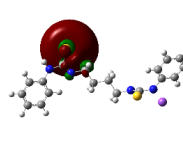
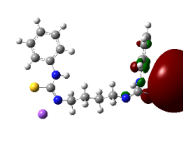
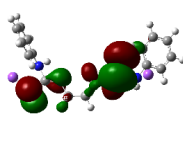
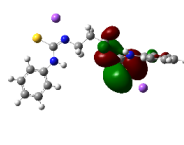
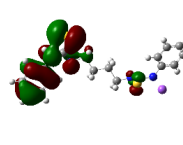
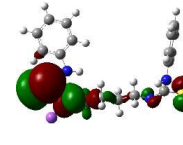
**Global reactivity indices of regioisomeric products (*Z/E*)-**1**** Theoretical calculations of the total energy (RB3LYP) [59] derived from conceptual DFT provide additional evidence for the superiority of (*Z*)-**1** over (*E*)-**1**. Global reactivity indices of (*Z/E*)-**1a** as a typical example are presented in Table 7 in three different media, namely gas, water, and ethanol. The findings of all products are presented in Tables S3–S5 in the electronic supplementary file.

As shown in Table 7, the total energies of (*Z*)-**1a** were lower than those of (*E*)-**1a**. Specifically, the values for (*Z*)-**1a** ranged from -1,436,875.846 to -1,436,866.015 kcal/mol, whereas the values for (*E*)-**1a** ranged from -1,436,861.814 to -1,436,850.865 kcal/mol.

**Theoretical energy differences calculations for the interaction of  $\alpha$ -haloketone **5** and (*Z*)-bis(carbamimidothioates) **7**** FMO analysis was used as an important step in understanding the mechanism of the regioselective reaction between  $\alpha$ -haloketones **5** and (*Z*)-bis(carbamimidothioates) **7**. Therefore, the calculation of the two possible relative



**Table 4** FMO of alkane-linked bis(carbamimidothioates) **7/8**

Reactant	(Z)- <b>7a</b>	(E)- <b>7a</b>	(Z)- <b>7b</b>	(E)- <b>7b</b>
Optimized structure				
LUMO				
$E_{\text{LUMO}}$ (eV)	-1.049	-1.342	-1.596	-1.608
HOMO				
$E_{\text{HOMO}}$ (eV)	-4.904	-4.868	-4.788	-4.937
Reactant	(Z)- <b>8a</b>	(E)- <b>8a</b>	(Z)- <b>8b</b>	(E)- <b>8b</b>
Optimized structure				
LUMO				
$E_{\text{LUMO}}$ (eV)	-1.399	-1.557	-1.589	-1.592
HOMO				
$E_{\text{HOMO}}$ (eV)	-4.802	-4.572	-4.996	-4.837



**Table 5** Global descriptors for  $\alpha$ -bromoketones **5** and alkane-linked bis(carbamimidothioates) **7/8**

Product	HOMO (eV)	LUMO (eV)	I (eV) <sup>a</sup>	A (eV) <sup>b</sup>	$\eta$ (eV) <sup>c</sup>	S <sup>d</sup>	$\mu$ (eV) <sup>e</sup>	$\omega$ (au/eV) <sup>f</sup>	N (eV) <sup>g</sup>	E (RB3LYP) (Kcal/mol)
<b>5a</b>	-7.374	-2.552	7.374	2.552	4.822	0.208	-4.963	2.554	2.034	-1,854,920.235
<b>5b</b>	-7.410	-2.645	7.410	2.645	4.765	0.210	-5.028	2.652	1.998	-2,143,307.714
<b>5c</b>	-6.708	-2.211	6.708	2.211	4.497	0.222	-4.460	2.211	2.700	-1,926,789.734
<b>5d</b>	-7.155	-3.113	7.155	3.113	4.042	0.247	-5.134	3.261	2.253	-2,021,061.705
<b>5e</b>	-7.181	-3.302	7.181	3.302	3.879	0.258	-5.242	3.542	2.227	-2,309,459.695
<b>5f</b>	-7.130	-3.309	7.130	3.309	3.821	0.262	-5.220	3.565	2.278	-3,634,451.887
(Z)- <b>7a</b>	-4.904	-1.049	4.904	1.049	3.855	0.259	-2.977	1.149	4.504	-1,254,254.710
(E)- <b>7a</b>	-4.868	-1.342	4.868	1.342	3.526	0.284	-3.105	1.367	4.540	-1,254,249.402
(Z)- <b>7b</b>	-4.788	-1.596	4.788	1.596	3.192	0.313	-3.192	1.596	4.908	-1,278,912.874
(E)- <b>7b</b>	-4.937	-1.608	4.937	1.609	3.328	0.301	-3.273	1.610	4.471	-1,278,911.847
(Z)- <b>8a</b>	-4.802	-1.399	4.802	1.399	3.403	0.294	-3.101	1.413	4.606	-1,254,230.28
(E)- <b>8a</b>	-4.572	-1.557	4.572	1.557	3.015	0.332	-3.065	1.557	4.836	-1,254,214.504
(Z)- <b>8b</b>	-4.996	-1.589	4.996	1.589	3.407	0.294	-3.293	1.591	4.412	-1,278,900.831
(E)- <b>8b</b>	-4.837	-1.592	4.837	1.592	3.245	0.308	-3.215	1.592	4.571	-1,278,900.322

<sup>a</sup>Ionization potential (I) =  $-E_{\text{HOMO}}$ ; <sup>b</sup>Electron affinity (A) =  $-E_{\text{LUMO}}$ ; <sup>c</sup>Global hardness ( $\eta$ ) =  $(I-A)$ ; <sup>d</sup>Softness (S) =  $1/\eta$ ; <sup>e</sup>Chemical potential ( $\mu$ ) =  $(E_{\text{HOMO}} + E_{\text{LUMO}})/2$ ; <sup>f</sup>Electrophilicity index ( $\omega$ ) =  $\mu^2/2\eta$ ; <sup>g</sup>Nucleophilicity index (N) =  $(E_{\text{HOMO}}(N_{\text{u}}) - E_{\text{HOMO}}(\text{TCE}))$

energy interactions  $\Delta E_1 [(E_{\text{LUMO}}(Z-7)) - (E_{\text{HOMO}}(5))]$  and  $\Delta E_2 [(E_{\text{LUMO}}(5)) - (E_{\text{HOMO}}(Z-7))]$  are shown in Table 8 [60].

Generally, we found that  $\Delta E_2$  is smaller than  $\Delta E_1$ . This implies that HOMO of (Z)-**7** interacts with LUMO of **5** to initiate the reaction. This result offers significant support for the hypothesis that electrons move from the more nucleophilic (Z)-bis(carbamimidothioates) **7** to the more electrophilic  $\alpha$ -haloketones **5**. The FMO diagram for the interaction between  $\alpha$ -haloketone **5a** and (Z)-bis(carbamimidothioates) **7a,b** is shown in Fig. 6. The  $\Delta E_1$  and  $\Delta E_2$  of the **5a/7a** interaction are 5.659 and 2.352 eV, respectively, whereas the  $\Delta E_1$  and  $\Delta E_2$  of the **5a/7b** interaction are 5.112 and 2.236 eV, respectively.

### Theoretical calculations of Parr indexes and local nucleophilicity and electrophilicity

Using local reactivity indices [61–67], the next step involves determining which of the nucleophilic centers from (Z)-**7** will be the most effective in attacking the highly electrophilic center in **5**. Recent advancements have turned the Parr, local nucleophilic, and local electrophilic indices into powerful tools for site selectivity [63, 68]. To compute the Parr function, the atomic spin density was analyzed under unrestricted formalization (UB3LYP) using the Gaussian 09 program and the 6–31 + G(d,p) basis set [64]. The preferred attack site can be identified by utilizing the Parr, local nucleophilic, and local electrophilic indices [69]. Tables 9 and 10 summarize the information obtained from these indices for both **5** and (Z)-**7**.

Based on data collected on Parr [64], and local nucleophilicity [65], as well as dual descriptors [63] for (Z)-**7a,b**, we have found that the sulfur site is more nucleophilic than the NH site. As an example, in **7a**, the local nucleophilicity ( $NP^-$ ) of the sulfur site is 0.721, which is higher than that of the NH site, which is only 0.027. Similarly, the Parr nucleophilicity ( $P_r^-$ ) of the sulfur site is higher with a value of 0.160 compared to the NH site with a value of 0.006. Moreover, the dual descriptor ( $\Delta f_r$ ) on the sulfur site is more negative than that on the NH site with values of  $-0.012$  and  $+0.028$ , respectively. Additionally, the local Fukui nucleophilicity ( $Nf_r^-$ ) of the sulfur site is more positive, with a value of  $+0.014$ , whereas the NH site has a value of  $-0.140$ .

We have determined that, based on our analysis of Parr [64], local electrophilicity [65], and dual descriptors [63] of compounds **5a–5f**, the  $\text{CH}_2$ -site adjacent to the bromine atom in the molecule is more electrophilic than the carbon-site of the carbonyl group. For instance, in **5a**, the local electrophilicity of the  $\text{CH}_2$ -site ( $\omega P^+$ ) is  $+1.540$ , which is higher than that of the CO-site ( $-0.158$ ), and the Parr electrophilicity ( $P^+$ ) of the  $\text{CH}_2$ -site ( $+0.603$ ) is also higher than that of the CO-site ( $-0.062$ ). Additionally, the dual descriptor ( $\Delta f_r$ ) value on the  $\text{CH}_2$ -site ( $+0.134$ ) is more positive than that on the CO-site ( $-0.144$ ), while the local Fukui electrophilicity ( $\omega f^+$ ) of the  $\text{CH}_2$ -site ( $+1.540$ ) is more positive than that of the CO-site ( $-0.158$ ). These findings demonstrate that the attack of the more nucleophilic sulfur site in (Z)-**7** on the more electrophilic  $\text{CH}_2$ -site in **5** will initiate the reaction (see Fig. 7).

**Table 6** FMO of the regioisomeric products (*Z/E*)-1

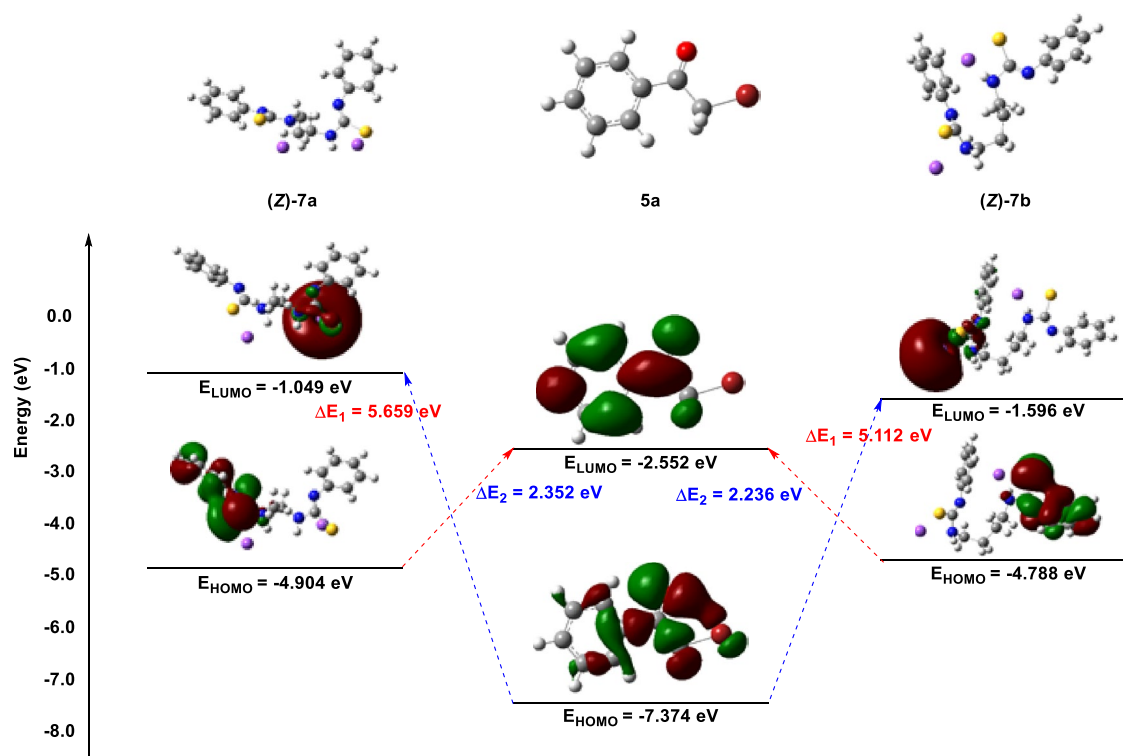
( <i>Z</i> )-1a	Gas	Water	EtOH
Optimized structure			
LUMO			
$E_{\text{LUMO}}$ (eV)	-0.831	-0.810	-0.804
HOMO			
$E_{\text{HOMO}}$ (eV)	-5.000	-5.195	-5.181
( <i>E</i> )-1a	Gas	Water	EtOH
Optimized structure			
LUMO			
$E_{\text{LUMO}}$ (eV)	-0.999	-0.883	-0.881
HOMO			
$E_{\text{HOMO}}$ (eV)	-5.105	-5.270	-5.258

**Table 7** Theoretical calculations for regioisomeric products (*Z/E*)-1

	Medium	HOMO (eV)	LUMO (eV)	I (eV) <sup>a</sup>	A (eV) <sup>b</sup>	$\eta$ (eV) <sup>c</sup>	S <sup>d</sup>	$\mu$ (eV) <sup>e</sup>	$\omega$ (au/eV) <sup>f</sup>	N (eV) <sup>g</sup>	E (RB3LYP) (Kcal/mol)
<b>(Z)-1a</b>	Gas	-5.000	-0.831	5.000	0.831	4.169	0.240	-2.916	1.020	4.121	-1,436,866.015
	Ethanol	-5.181	-0.804	5.181	0.804	4.377	0.229	-2.993	1.023	3.940	-1,436,875.324
	Water	-5.195	-0.81	5.195	0.810	4.385	0.228	-3.003	1.028	3.926	-1,436,875.846
<b>(E)-1a</b>	Gas	-5.105	-0.999	5.105	0.999	4.106	0.244	-3.052	1.134	4.016	-1,436,850.865
	Ethanol	-5.258	-0.881	5.258	0.881	4.377	0.229	-3.070	1.076	3.863	-1,436,861.202
	Water	-5.270	-0.883	5.270	0.883	4.387	0.228	-3.077	1.079	3.851	-1,436,861.814

**Table 8** Theoretical calculations of energy differences ( $\Delta E_1$  and  $\Delta E_2$ ) for the interaction between  $\alpha$ -haloketones **5** and (*Z*)-bis(carbamimidothioates) **7**

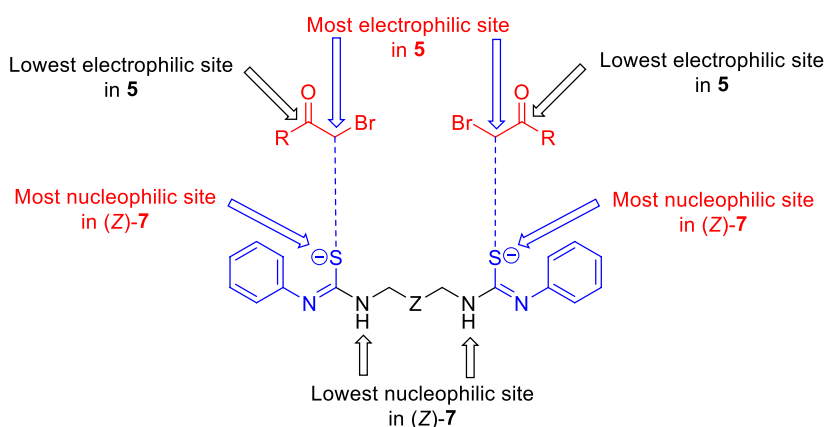
Reactant	<b>5a</b>	<b>5b</b>	<b>5c</b>	<b>5d</b>	<b>5e</b>	<b>5f</b>
$\Delta E_1$ ( <i>57a</i> ) (eV)	5.659	6.361	6.325	6.081	6.132	6.106
$\Delta E_2$ ( <i>57a</i> ) (eV)	2.352	2.259	2.693	1.595	1.602	1.791
$\Delta E_1$ ( <i>57b</i> ) (eV)	5.112	5.814	5.778	5.534	5.585	5.559
$\Delta E_2$ ( <i>57b</i> ) (eV)	2.236	2.143	2.577	1.479	1.486	1.675

**Fig. 6** FMO diagram for the interaction between  $\alpha$ -haloketones **5** and (*Z*)-bis(carbamimidothioates) **7****Table 9** Dual descriptor and Parr and local nucleophilicity indices of (*Z*)-**7a, b**

	Site	$P_r^-$	$f_r^+$	$f_r^-$	$\Delta f_r$	$NP_r^-$	$Nf_r^-$
<b>(Z)-7a</b>	S-site	0.160	-0.009	0.003	-0.012	0.721	0.014
	NH-site	0.006	-0.003	-0.031	0.028	0.027	-0.140
<b>(Z)-7b</b>	S-site	0.118	-0.006	0.048	-0.054	0.579	0.221
	NH-site	0.022	0.007	-0.057	0.064	0.108	-0.263

**Table 10** Dual descriptor and Parr and local electrophilicity indices of **5**

	Site	$P_r^+$	$f_r^+$	$f_r^-$	$\Delta f_r$	$\omega$	$\omega P_r^+$	$\omega f_r^+$
<b>5a</b>	CH <sub>2</sub> -site	0.603	0.165	0.031	0.134	2.554	1.540	1.540
	CO-site	-0.062	-0.152	-0.008	-0.144		-0.158	-0.158
<b>5b</b>	CH <sub>2</sub> -site	0.584	0.162	0.026	0.136	2.652	1.549	1.549
	CO-site	-0.062	-0.153	0.006	-0.1159		-0.164	-0.164
<b>5c</b>	CH <sub>2</sub> -site	0.628	0.166	0.016	0.150	2.211	1.389	1.389
	CO-site	-0.074	-0.142	0.008	-0.150		-0.164	-0.164
<b>5d</b>	CH <sub>2</sub> -site	0.504	0.018	0.01	0.008	3.261	1.644	0.059
	CO-site	-0.065	-0.055	-0.02	-0.035		-0.212	-0.179
<b>5e</b>	CH <sub>2</sub> -site	0.476	0.017	0.012	0.005	3.541	1.686	0.060
	CO-site	-0.064	-0.052	-0.028	-0.025		-0.227	-0.184
<b>5f</b>	CH <sub>2</sub> -site	0.477	0.016	0.011	0.005	3.565	1.701	0.057
	CO-site	-0.064	-0.051	-0.029	-0.022		-0.228	-0.182

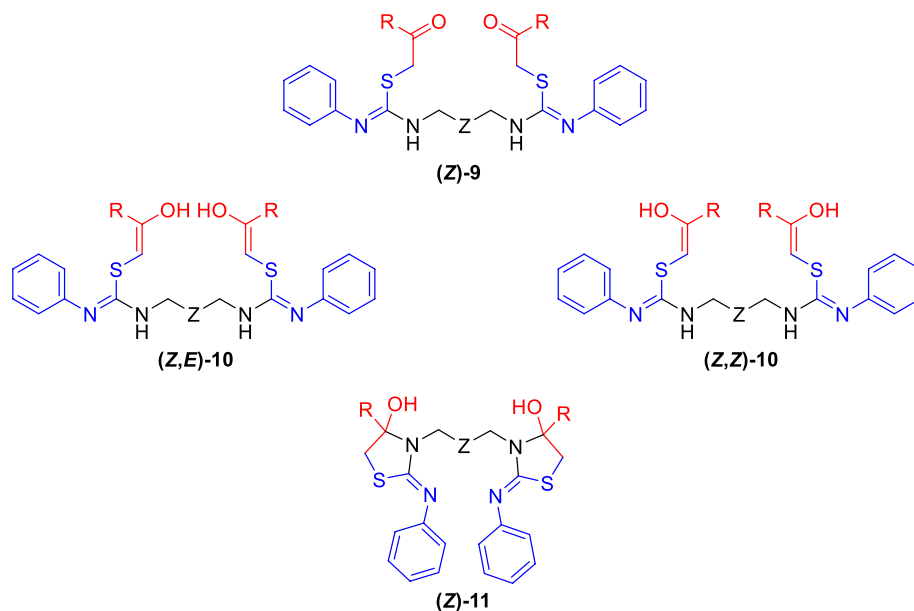
**Fig. 7** Favorable reaction pathway between **5** and (Z)-**7**

### Theoretical calculations for the proposed intermediates **9–11**

Further study of the reaction between **5** and (Z)-**7** was performed by computing global descriptors of the proposed intermediates [56–58, 70, 71]. The previous calculations were used to predict the plausible mechanism of the formation of the target hybrids **1**. As previously discussed, the reaction between **5** and (Z)-**7** can be triggered by the nucleophilic substitution reaction between the sulfur-site in (Z)-**7** and the electrophilic CH<sub>2</sub> adjacent to the bromine atom in **5**, resulting in the corresponding (Z)-bis(S-alkyl) derivative **9**. This intermediate may then be converted into three possible intermediates: (Z,Z)-**10**, (Z,E)-**10** or (Z)-**11**. The compound (Z)-**9** can tautomerize to either (Z,Z)-**10** or (Z,E)-**10** in their enol-forms. Furthermore, (Z)-**9** can undergo cyclization via the acyl nucleophilic addition of the two spacer-NH sites to the carbonyl functions, forming the adduct (Z)-**11** (see Fig. 8).

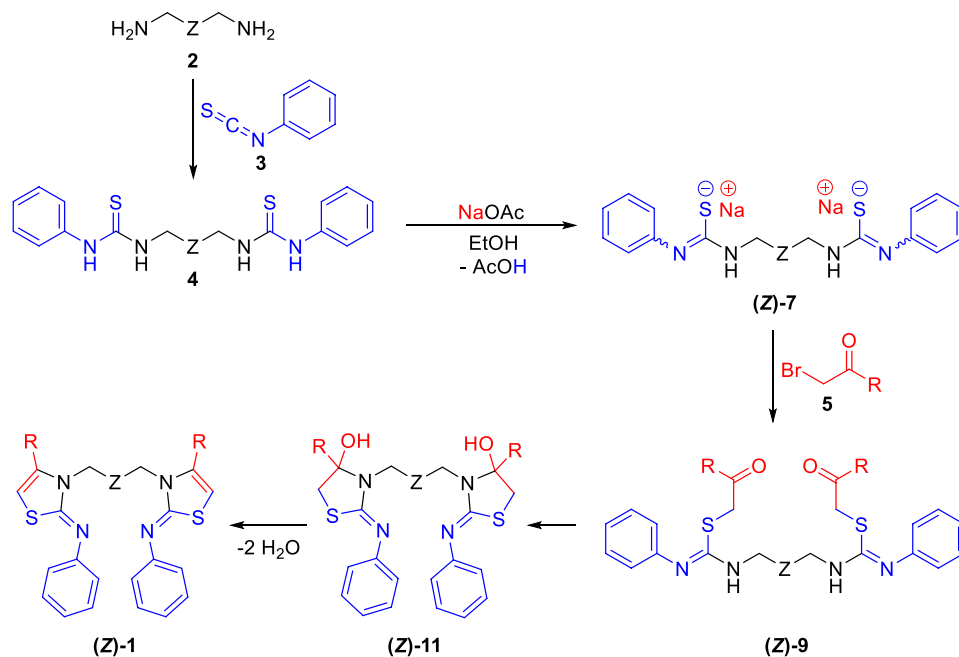
Calculating the energy of compounds (Z,Z)-**10**, (Z,E)-**10**, and (Z)-**11** leads us to anticipate which route compound (Z)-**9** will take. Taking the reaction between **5a** and (Z)-**7a** as a model, the theoretical parameters for the intermediates **9–11** are listed in Table 11. All calculations are listed in Table S6 in the electronic supplementary file. It is evident from the data gathered for **10** and **11** that cyclization is preferable than tautomerization in all derivatives.

Based on the aforementioned findings, the mechanism for the current three-component reaction can be summarized in Scheme 7. First, alkane-linked diamines **2** were reacted with phenyl isothiocyanate **3** to yield bis(3-phenylthiourea) derivatives **4**. The previous intermediate produces the most stable (Z)-bis(carbamimidothioates) **7** in the presence of sodium acetate, which then reacted with  $\alpha$ -haloketones **5** via a nucleophilic substitution reaction to give the corresponding (Z)-bis(S-alkyl) derivative **9**. The acyl nucleophilic additions of the two spacer-NH sites to the carbonyl functions produced the adduct (Z)-**11**. Next, two molecules of water were removed from (Z)-**11** to yield the regioisomeric (Z)-**1** as a final isolable product.

**Fig. 8** Structure of the proposed intermediates **9–11****Table 11** Global descriptors for intermediates **9–11**

	HOMO (eV)	LUMO (eV)	I (eV) <sup>a</sup>	A (eV) <sup>b</sup>	$\eta$ (eV) <sup>c</sup>	S <sup>d</sup>	$\mu$ (eV) <sup>e</sup>	$\omega$ (au/eV) <sup>f</sup>	N (eV) <sup>g</sup>	E (RB3LYP) (Kcal/mol)
(Z)-9	-5.265	-2.162	5.265	2.162	3.103	0.322	-3.714	2.222	3.856	-1,532,794.281
(Z,Z)-10	-5.269	-1.439	5.269	1.439	3.83	0.261	-3.354	1.469	3.852	-1,532,775.128
(Z,E)-10	-5.267	-1.212	5.267	1.212	4.055	0.247	-3.240	1.294	3.854	-1,532,768.004
(Z)-11	-5.498	-0.626	5.498	0.626	4.872	0.205	-3.062	0.962	3.623	-1,532,795.781

<sup>a</sup>Ionization potential (I) =  $-E_{\text{HOMO}}$ ; <sup>b</sup>Electron affinity (A) =  $-E_{\text{LUMO}}$ ; <sup>c</sup>Global hardness ( $\eta$ ) = (I-A); <sup>d</sup>Softness (S) =  $1/\eta$ ; <sup>e</sup>Chemical potential ( $\mu$ ) =  $(E_{\text{HOMO}} + E_{\text{LUMO}})/2$ ; <sup>f</sup>Electrophilicity index ( $\omega$ ) =  $\mu^2/2\eta$ ; <sup>g</sup>Nucleophilicity index (N) =  $(E_{\text{HOMO}}(\text{Nu}) - E_{\text{HOMO}}(\text{TCE}))$

**Scheme 7** Plausible mechanism for the formation of the (Z)-bis(*N*-phenylthiazol-2(3*H*)-imines) **1**

## Conclusion

A new series of (*Z*)-bis(*N*-phenylthiazol-2(*3H*)-imines) was efficiently prepared using a three-component protocol. For this purpose, a one-pot reaction was conducted between alkane-linked diamines, phenyl isothiocyanate, and the appropriate  $\alpha$ -bromoketones in ethanol in the presence of anhydrous sodium acetate. Both 1D and 2D NMR techniques were used to investigate the regioselectivity of the one-pot reaction as well as the assigned structure of new products. Additional support for the aforementioned findings was obtained by DFT-based calculations at the computational level B3LYP/6–31 + G(d,p). The current study demonstrated that the favored mechanism and experimental regioselectivity of the applied reaction protocol, as well as the assigned configuration of new products, could be correctly predicted using previous computational tools.

## Experimental

### Materials

All solvents unless otherwise noted, were purchased from commercial sources and utilized directly as received. The other substances were purchased from Merck or Aldrich and utilized directly. The melting points are uncorrected and determined using Stuart's melting point equipment. IR spectra were recorded using the Nicolet iS10 FT-IR spectrometer's Smart iTR. Chemical shifts were represented as ppm units, and NMR spectra were captured on a Bruker Avance III 400 MHz spectrophotometer (400 MHz for  $^1\text{H}$  and 100 MHz for  $^{13}\text{C}$ ) using TMS as an internal standard and DMSO- $d_6$  as a solvent. Elemental analyses were performed on a EuroVector instrument C, H, N analyzer EA3000 Series. For detailed synthetic protocol and characterization data of all newly synthesized products, see the Electronic supplementary file.

### Typical procedure for tandem synthesis of alkane-linked bis(*N*-phenylthiazol-2(*3H*)-imine) hybrids 1

A mixture of alkane-linked diamine **2a,b** (1 mmol), phenyl isothiocyanate **3** (2 mmol), and the appropriate  $\alpha$ -bromoketones **5a–5f** (2 mmol) was heated in ethanol (15 mL) in the presence of anhydrous sodium acetate (2.2 mmol) at 80 °C for 3–5 h. The reaction mixture was cooled and the obtained product was collected by filtration, washed with cold water, dried and recrystallized from the appropriate solvent.

## Computational screening

The theoretical calculations were carried out using the Gaussian 09W software [56, 57]. Using the widely accepted 6–31 + G(d,p) basis set, the molecular geometry of the investigated compounds was optimized using the density functional theory B3LYP approach. The optimized structure was visualized with GaussView 6.0.1 [58, 70, 71].

### Frontier molecular orbitals and global reactivity indices

The HOMO (highest-occupied molecular orbital) and LUMO (lowest-unoccupied molecular orbital) were estimated at the same computational level. Measurements are performed to define a system's reactivity and stability using widely applied chemical principles generated from conceptual DFT (see Electronic supplementary file) [72–78].

### Local reactivity indexes

To describe the regioselectivity of an atom 'r' in a molecule, several local reactivity indices are computed, including the condensed Fukui functions ( $f_r^+$  and  $f_r^-$ ) [61, 62], the dual descriptor ( $\Delta f_r$ ) [63], Parr functions ( $P_r$ ) [64, 65], and Domingo-related work (see Electronic supplementary file) [66, 67].

**Supplementary Information** The online version contains supplementary material available at <https://doi.org/10.1007/s13738-023-02851-5>.

**Funding** Open access funding provided by The Science, Technology & Innovation Funding Authority (STDF) in cooperation with The Egyptian Knowledge Bank (EKB).

**Open Access** This article is licensed under a Creative Commons Attribution 4.0 International License, which permits use, sharing, adaptation, distribution and reproduction in any medium or format, as long as you give appropriate credit to the original author(s) and the source, provide a link to the Creative Commons licence, and indicate if changes were made. The images or other third party material in this article are included in the article's Creative Commons licence, unless indicated otherwise in a credit line to the material. If material is not included in the article's Creative Commons licence and your intended use is not permitted by statutory regulation or exceeds the permitted use, you will need to obtain permission directly from the copyright holder. To view a copy of this licence, visit <http://creativecommons.org/licenses/by/4.0/>.

## References

1. M. Shiri, Chem. Rev. **112**, 3508–3549 (2012). <https://doi.org/10.1021/cr2003954>
2. S. Moghimi, M. Shiri, M.M. Heravi, H.G. Kruger, Tetrahedron Lett. **54**, 6215–6217 (2013). <https://doi.org/10.1016/j.tetlet.2013.09.008>
3. R.C. Cioc, E. Ruijter, R.V. Orru, Green Chem. **16**, 2958–2975 (2014). <https://doi.org/10.1039/C4GC00013G>



4. C.C. Meyer, E. Ortiz, M.J. Krische, *Chem. Rev.* **120**, 3721–3748 (2020). <https://doi.org/10.1021/acs.chemrev.0c00053>
5. Y. Huang, A. Dömling, *Mol. Divers.* **15**, 3–33 (2011). <https://doi.org/10.1007/s11030-010-9229-6>
6. O. Ghashghaei, C. Masdeu, C. Alonso, F. Palacios, R. Lavilla, *Drug Discov. Today Technol.* **29**, 71–79 (2018). <https://doi.org/10.1016/j.ddtec.2018.08.004>
7. I. Ugi, A. Demharter, W. Hörl, T. Schmid, *Tetrahedron* **52**, 11657–11664 (1996). [https://doi.org/10.1016/0040-4020\(96\)00647-3](https://doi.org/10.1016/0040-4020(96)00647-3)
8. P. Wu, M. Givskov, T.E. Nielsen, *Chem. Rev.* **119**, 11245–11290 (2019). <https://doi.org/10.1021/acs.chemrev.9b00214>
9. S.M.H. Sanad, A.E.M. Mekky, A.A.M. Ahmed, *ChemistrySelect* **8**, e202300171 (2023). <https://doi.org/10.1002/slct.202300171>
10. S.M.H. Sanad, A.A.M. Abdelsalam, A.A. Gamal Eldin, E.H. Abdelfattah, F.R.M. Hussein, N.G. Mohammed, N.A.S. Taha, A.E.M. Mekky, *Chem. Biodivers.* (2023). <https://doi.org/10.1002/cbdv.202300546>
11. S. Rezaayati, F. Kalantari, A. Ramazani, S. Sajjadifar, H. Aghahosseini, A. Rezaei, *Inorg. Chem.* **61**, 992–1010 (2022). <https://doi.org/10.1021/acs.inorgchem.1c03042>
12. Z. Hosseinzadeh, A. Ramazani, N. Razzaghi-Asl, *Curr. Org. Chem.* **22**, 2256–2279 (2018). <https://doi.org/10.2174/1385272822666181008142138>
13. A. Ramazani, A.T. Mahyari, M. Rouhani, A. Rezaei, *Tetrahedron Lett.* **50**, 5625–5627 (2009). <https://doi.org/10.1016/j.tetlet.2009.07.115>
14. A. Souldozi, A. Ramazani, N. Bouslimani, R. Welter, *Tetrahedron Lett.* **48**, 2617–2620 (2007). <https://doi.org/10.1016/j.tetlet.2007.02.010>
15. Z.A. Abdallah, S.M.H. Sanad, A.E.M. Mekky, M.S.M. Ahmed, *Chem. Biodivers.* **20**, e202300206 (2023). <https://doi.org/10.1016/10.1002/cbdv.202300206>
16. S.K.J. Shaikh, R.R. Kamble, S.M. Somagond, A.A. Kamble, M.N. Kumbar, *Synth. Commun.* **48**, 2061–2073 (2018). <https://doi.org/10.1080/00397911.2018.1482348>
17. S. Aamer, Z. Sabah, J. Maryam, M. Bushra, *Turk. J. Chem.* **32**, 585–592 (2008)
18. S.M. Sondhi, A.D. Dwivedi, J. Singh, P.P. Gupta, *Indian J. Chem.* **49B**, 1076–1082 (2010)
19. S.M. Sondhi, N. Singh, A.M. Lahoti, K. Bajaj, A. Kumar, O. Lozach, L. Meijer, *Bioorg. Med. Chem.* **13**, 4291–4299 (2005). <https://doi.org/10.1016/j.bmc.2005.04.017>
20. A. Manaka, M. Sato, M. Aoki, M. Tanaka, T. Ikeda, Y. Toda, Y. Yamane, S. Nakaike, *Bioorg. Med. Chem.* **11**, 1031–1035 (2001). [https://doi.org/10.1016/S0960-894X\(01\)00123-8](https://doi.org/10.1016/S0960-894X(01)00123-8)
21. H. Eshghi, F. Eshkil, A.S. Saljooghi, M. Bakavoli, *Org. Chem. Res.* **5**, 87–94 (2019). <https://doi.org/10.22036/org.chem.2018.133272.1148>
22. R. Mudavath, B. Ushaiah, C.K. Prasad, K. Sudeepa, P. Ravindar, S.N.T. Sunitha, C.S. Devi, *J. Biomol. Struct. Dyn.* **38**, 2849–2864 (2020). <https://doi.org/10.1080/07391102.2019.1647878>
23. D.S. Kim, Y.M. Jeong, I.K. Park, H.G. Hahn, H.K. Lee, S.B. Kwon, J.H. Jeong, S.J. Yang, U.D. Sohn, K.C. Park, *Biol. Pharm. Bull.* **30**, 180–183 (2007). <https://doi.org/10.1248/bpb.30.180>
24. A.E.M. Mekky, S.M.H. Sanad, T.T. El-Idreesy, *Synth. Commun.* **51**, 3332–3344 (2021). <https://doi.org/10.1080/00397911.2021.1970774>
25. A. Hantzsch, J.H. Weber, *Ber. Chem. Gesellschaf.* **20**, 3118–3132 (1887). <https://doi.org/10.1002/cber.188702002200>
26. S.M.H. Sanad, A.E.M. Mekky, *Synth. Commun.* **51**, 611–624 (2021). <https://doi.org/10.1080/00397911.2020.1846748>
27. S.M.H. Sanad, A.E.M. Mekky, A.Y. Said, M.A.A. Elneairy, *J. Heterocycl. Chem.* **58**, 1461–1471 (2021). <https://doi.org/10.1002/jhet.4272>
28. A.E.M. Mekky, S.M.H. Sanad, *J. Heterocycl. Chem.* **56**, 1560–1566 (2019). <https://doi.org/10.1002/jhet.3531>
29. J. Safari, Z. Abedi-Jazini, Z. Zarnegar, M. Sadeghi, *Catal. Commun.* **77**, 108–112 (2016). <https://doi.org/10.1016/j.catcom.2016.01.007>
30. R. Raja, D. Murugan, A. Sivasubramaniyan, J. George, S. Perumal, P. Alagusundaram, M.R. Jayakumar, M. Saminathan, *Synth. Commun.* **46**, 942–948 (2016). <https://doi.org/10.1080/00397911.2016.1178775>
31. K. Appalanaidu, T. Dadmal, N.J. Babu, R.M. Kumbhare, *RSC Adv.* **5**, 88063–88069 (2015). <https://doi.org/10.1039/C5RA17278K>
32. M.M. Heravi, S. Moghimi, *Tetrahedron Lett.* **53**, 392–394 (2012). <https://doi.org/10.1016/j.tetlet.2011.11.017>
33. G.W. Kabalka, A.R. Mereddy, *Tetrahedron Lett.* **47**, 5171–5172 (2006). <https://doi.org/10.1016/j.tetlet.2006.05.053>
34. A.S. Shahvelayati, I. Yavari, A.S. Delbari, *Chin. Chem. Lett.* **25**, 119–122 (2014). <https://doi.org/10.1016/j.ccllet.2013.11.009>
35. G.S. Kumar, S.P. Ragini, H.M. Meshram, *Tetrahedron Lett.* **54**, 5974–5978 (2013). <https://doi.org/10.1016/j.tetlet.2013.08.056>
36. G.S. Kumar, A.S. Kumar, H.M. Meshram, *Synlett* **27**, 399–403 (2016). <https://doi.org/10.1055/s-0035-1560502>
37. A. Miloudi, D. El-Abed, G. Boyer, J.P. Finet, J.P. Galy, D. Siri, *Eur. J. Org. Chem.* **2004**, 1509–1516 (2004). <https://doi.org/10.1002/ejoc.200300656>
38. N. De Kimpe, M. Boelens, J.P. Declercq, *Tetrahedron* **49**, 3411–3424 (1993). [https://doi.org/10.1016/S0040-4020\(01\)90168-1](https://doi.org/10.1016/S0040-4020(01)90168-1)
39. J. Svetlik, F. Turecek, I. Goljer, *J. Org. Chem.* **55**, 4740–4744 (1990). <https://doi.org/10.1021/jo00302a048>
40. J. Liebscher, E. Mitzner, *Tetrahedron Lett.* **26**, 1835–1838 (1985). [https://doi.org/10.1016/S0040-4039\(00\)94750-6](https://doi.org/10.1016/S0040-4039(00)94750-6)
41. F. Tittelbach, S. Vieth, M. Schneider, *Eur. J. Org. Chem.* **1998**, 515–520 (1998). [https://doi.org/10.1002/\(SICI\)1099-0690\(199803\)1998:3%3c515::AID-EJOC515%3e3.0.CO;2-6](https://doi.org/10.1002/(SICI)1099-0690(199803)1998:3%3c515::AID-EJOC515%3e3.0.CO;2-6)
42. M. Dhooghe, A. Waterinckx, N. De Kimpe, *J. Org. Chem.* **70**, 227–232 (2005). <https://doi.org/10.1021/jo048486f>
43. Y. Sanemitsu, S. Kawamura, J. Satoh, T. Katayama, S. Hashimoto, *J. Pestic. Sci.* **31**, 305–310 (2006). <https://doi.org/10.1584/jpestics.31.305>
44. A.A.M. Ahmed, A.E.M. Mekky, S.M.H. Sanad, *J. Heterocycl. Chem.* (2023). <https://doi.org/10.1002/jhet.4688>
45. A.E.M. Mekky, N.A.S. Taha, N.G. Mohammed, F.R.M. Hussein, E.H. Abdelfattah, A.A. Gamal Eldin, A.A.M. Abdelsalam, S.M.H. Sanad, *Synth. Commun.* **53**, 1053–1068 (2023). <https://doi.org/10.1080/00397911.2023.2209815>
46. S.M.H. Sanad, A.E.M. Mekky, *Synth. Commun.* **53**, 994–1007 (2023). <https://doi.org/10.1080/00397911.2023.2204192>
47. M.A.A. Elneairy, S.M.H. Sanad, A.E.M. Mekky, *Synth. Commun.* **53**, 245–261 (2023). <https://doi.org/10.1080/00397911.2022.2163506>
48. A.E.M. Mekky, S.M.H. Sanad, *ChemistrySelect* **8**, e202300487 (2023). <https://doi.org/10.1002/slct.202300487>
49. S.M.H. Sanad, M.S.M. Ahmed, A.E.M. Mekky, Z.A. Abdallah, *J. Mol. Struct.* **1243**, 130802 (2021). <https://doi.org/10.1016/j.molstruc.2021.130802>
50. A.E.M. Mekky, S.M.H. Sanad, *Chem. Biodivers.* **20**, 202200518 (2023). <https://doi.org/10.1002/cbdv.202200518>
51. S. Kavitha, N. Zulfreen, K. Kannan, S. Gnanavel, *Int. Res. J. Pharm.* **7**, 92–96 (2016). <https://doi.org/10.7897/2230-8407.0711135>
52. H.M. Abd El-Lateef, Z.A. Abdallah, M.S.M. Ahmed, *J. Mol. Liq.* **296**, 111800 (2019). <https://doi.org/10.1016/j.molliq.2019.111800>
53. P.B. Pansuriya, H.M. Parekh, H.B. Friedrich, G.E. Maguire, *J. Therm. Anal. Calorim.* **111**, 597–603 (2013). <https://doi.org/10.1007/s10973-012-2309-3>



54. S. Murru, C.B. Singh, V. Kavala, B.K. Patel, *Tetrahedron* **64**, 1931–1942 (2008). <https://doi.org/10.1016/j.tet.2007.11.076>
55. H. Osman, S.K. Yusufzai, M.S. Khan, B.M. Abd Razik, O. Sulaiman, S. Mohamad, J.A. Gansau, M.O. Ezzat, T. Parumasivam, M.Z. Hassan, *J. Mol. Struct.* **1166**, 147–154 (2018). <https://doi.org/10.1016/j.molstruc.2018.04.031>
56. A.D. Becke, *J. Chem. Phys.* **98**, 1372–1377 (1993). <https://doi.org/10.1063/1.464304>
57. Gaussian 09, Revision A.02, M.J. Frisch, G.W. Trucks, H.B. Schlegel, G.E. Scuseria, M.A. Robb, J.R. Cheeseman, G. Scalmani, V. Barone, B. Mennucci, G.A. Petersson, H. Nakatsuji, M. Caricato, X. Li, H.P. Hratchian, A.F. Izmaylov, J. Bloino, G. Zheng, J.L. Sonnenberg, M. Hada, M. Ehara, K. Toyota, R. Fukuda, J. Hasegawa, M. Ishida, T. Nakajima, Y. Honda, O. Kitao, H. Nakai, T. Vreven, J.A. Montgomery Jr., J.E. Peralta, F. Ogliaro, M. Bearpark, J.J. Heyd, E. Brothers, K.N. Kudin, V.N. Staroverov, T. Keith, R. Kobayashi, J. Normand, K. Raghavachari, A. Rendell, J.C. Burant, S.S. Iyengar, J. Tomasi, M. Cossi, N. Rega, J.M. Millam, M. Klene, J.E. Knox, J.B. Cross, V. Bakken, C. Adamo, J. Jaramillo, R. Gomperts, R.E. Stratmann, O. Yazyev, A.J. Austin, R. Cammi, C. Pomelli, J.W. Ochterski, R.L. Martin, K. Morokuma, V.G. Zakrzewski, G.A. Voth, P. Salvador, J.J. Dannenberg, S. Dapprich, A.D. Daniels, O. Farkas, J.B. Foresman, J.V. Ortiz, J. Cioslowski, D.J. Fox (Gaussian Inc., Wallingford CT, 2016)
58. C. Lee, W. Yang, R.G. Parr, *Phys. Rev. B* **37**, 785–789 (1988). <https://doi.org/10.1103/PhysRevB.37.785>
59. A. Georgiev, E. Bubev, D. Dimov, D. Yancheva, I. Zhivkov, J. Krajčovič, M. Vala, M. Weiter, M. Machkova, *Spectrochim. Acta Part A* **175**, 76–91 (2017). <https://doi.org/10.1016/j.saa.2016.12.005>
60. R.G. Pearson, *Inorg. Chem.* **27**, 734–740 (1988). <https://doi.org/10.1021/ic00277a030>
61. P.W. Ayers, R.G. Parr, *J. Am. Chem. Soc.* **122**, 2010–2018 (2000). <https://doi.org/10.1021/ja9924039>
62. R.G. Parr, W. Yang, *J. Am. Chem. Soc.* **106**, 4049–4050 (1984). <https://doi.org/10.1021/ja00326a036>
63. C. Morell, A. Grand, A. Toro-Labbé, *J. Phys. Chem. A* **109**, 205–212 (2005). <https://doi.org/10.1021/jp046577a>
64. L.R. Domingo, P. Pérez, J.A. Saéz, *RSC Adv.* **3**, 1486–1494 (2013). <https://doi.org/10.1039/C2RA22886F>
65. P. Pérez, L.R. Domingo, M. Duque-Norena, E. Chamorro, *J. Mol. Struct. THEOCHEM* **895**, 86–91 (2009). <https://doi.org/10.1016/j.theochem.2008.10.014>
66. L.R. Domingo, M.J. Aurell, P. Pérez, R. Contreras, *J. Phys. Chem. A* **106**, 6871–6875 (2002). <https://doi.org/10.1021/jp020715j>
67. W. Yang, W.J. Mortier, *J. Am. Chem. Soc.* **108**, 5708–5711 (1986). <https://doi.org/10.1021/ja00279a008>
68. L.R. Domingo, P. Pérez, J.A. Sáez, *Tetrahedron* **69**, 107–114 (2013). <https://doi.org/10.1016/j.tet.2012.10.056>
69. P. Politzer, J. Murray, *Theor. Chem. Acc.* **108**, 134–142 (2002). <https://doi.org/10.1007/s00214-002-0363-9>
70. A.D. Becke, *J. Chem. Phys.* **98**, 5648–5652 (1993). <https://doi.org/10.1063/1.464913>
71. R. Ditchfield, W.J. Hehre, J.A. Pople, *J. Chem. Phys.* **54**, 724–728 (1971). <https://doi.org/10.1063/1.1674902>
72. R.G. Pearson, *J. Am. Chem. Soc.* **108**, 6109–6114 (1986). <https://doi.org/10.1021/ja00280a002>
73. R.G. Pearson, J. Songstad, *J. Am. Chem. Soc.* **89**, 1827–1836 (1967). <https://doi.org/10.1021/ja00984a014>
74. R.G. Parr, R.G. Pearson, *J. Am. Chem. Soc.* **105**, 7512–7516 (1983). <https://doi.org/10.1021/ja00364a005>
75. A. Vela, J.L. Gazquez, *J. Am. Chem. Soc.* **112**, 1490–1492 (1990). <https://doi.org/10.1021/ja00160a029>
76. A. Toro-Labbé, *J. Phys. Chem. A* **103**, 4398–4403 (1999). <https://doi.org/10.1021/jp984187g>
77. R.G. Parr, L.V. Szentpály, S. Liu, *J. Am. Chem. Soc.* **121**, 1922–1924 (1999). <https://doi.org/10.1021/ja983494x>
78. L.R. Domingo, E. Chamorro, P. Pérez, *J. Org. Chem.* **73**, 4615–4624 (2008). <https://doi.org/10.1021/jo800572a>